

Electron-phonon interaction in the normal and superconducting states of MgB₂

Y. Kong, O.V. Dolgov, O. Jepsen, and O.K. Andersen
Max-Planck-Institut für Festkörperforschung,
Stuttgart, Germany
 (October 30, 2018)

For the 40K-superconductor MgB₂ we have calculated the electronic and phononic structures and the electron-phonon interaction throughout the Brillouin zone *ab initio*. In contrast to the isoelectronic graphite, MgB₂ has holes in the bonding σ -bands, which contribute 42 per cent to the density of states: $N(0) = 0.355$ states/(MgB₂·eV·spin). The total interaction strength, $\lambda = 0.87$ and $\lambda_{tr} = 0.60$, is dominated by the coupling of the σ -holes to the bond-stretching optical phonons with wavenumbers in a narrow range around 590 cm⁻¹. Like the holes, these phonons are quasi two-dimensional and have wave-vectors close to Γ A, where their symmetry is E. The π -electrons contribute merely 0.25 to λ and to λ_{tr} . With Eliashberg theory we evaluate the normal-state resistivity, the density of states in the superconductor, and the B-isotope effect on T_c and Δ_0 , and find excellent agreement with experiments, when available. $T_c=40$ K is reproduced with $\mu^* = 0.10$ and $2\Delta_0/k_B T_c = 3.9$. MgB₂ thus seems to be an intermediate-coupling e-ph pairing s -wave superconductor.

The recent discovery¹ of superconductivity with $T_c=39$ K in the graphite-like compound MgB₂ has caused hectic activity. Density-functional (LDA) calculations^{2–5} show that, in contrast to intercalated graphite ($T_c \leq 5$ K) and alkali-doped fullerenes, A₃C₆₀ ($T_c < 40$ K), in MgB₂ there are holes at the top of the B-B bonding σ -bands, and that these couple rather strongly to optical B-B bond-stretching modes⁵ with wavenumbers^{2,4} around 600 cm⁻¹. These are the same type of modes as those believed to couple most strongly to the π -electrons in graphite and C₆₀, where their wavenumbers are 2.5 times larger, however^{6,7}. Rough estimates^{2,5} of the electron-phonon coupling-strength for s -wave pairing in MgB₂ yield: $\lambda \sim 1$. Measurements of the B-isotope effect⁸ on T_c , tunnelling⁹, transport^{10–13}, thermodynamic properties^{10,14,15}, and the phonon density of states^{16,17} confirm that MgB₂ is most likely an electron-phonon mediated s -wave superconductor with intermediate^{9,14,17} or strong¹⁵ coupling.

In order to advance, detailed comparisons between accurate results of Eliashberg theory and experiments are needed. Consider again the example of A₃C₆₀, also believed to be conventional s -wave superconductors⁷ with T_c 's described by the McMillan expression:

$$T_c^{McM} = \frac{\omega_{ln}}{1.2} \exp \left[\frac{-1.04(1 + \lambda)}{\lambda - (1 + 0.62\lambda)\mu^*} \right]. \quad (1)$$

The LDA values for λ are 0.4–0.6 and the value of the Coulomb pseudopotential μ^* to be used in (1) is presumably considerably larger than the usual value, 0.1–0.2, for sp -materials¹⁸ due to the small width (~ 0.5 eV) of the π t_{1u} -subband compared with the on-ball Coulomb repulsion⁷. For MgB₂, where the π -band is 15 eV broad, one expects μ^* to be 0.1–0.2 and the LDA¹⁹ plus generalized-gradient correction²⁰ to give λ with an accuracy better than 0.1. The result of such a λ -

calculation will be presented here and should allow us to reach conclusions about the superconductivity in MgB₂.

MgB₂ consists of graphite-like B₂-layers stacked on-top with Mg in-between. The primitive translations are: $\mathbf{a}=(\sqrt{3}/2, 1/2, 0)a$, $\mathbf{b}=(0, a, 0)$, $\mathbf{c}=(0, 0, c)$, with²¹ $a = 3.083\text{\AA} = 5.826 a_0$ and $c/a = 1.142$. In reciprocal space, and in units of $2\pi/a$, the primitive translations are: $\mathbf{A}=(2/\sqrt{3}, 0, 0)$, $\mathbf{B}=(-1/\sqrt{3}, 1, 0)$, $\mathbf{C}=(0, 0, a/c)$, and the points of high symmetry are: $\Gamma=(0, 0, 0)$, $\mathbf{A}=(0, 0, a/2c)$, $\mathbf{M}=(1/\sqrt{3}, 0, 0)$, $\mathbf{L}=(1/\sqrt{3}, 0, a/2c)$, $\mathbf{K}=(1/\sqrt{3}, 1/3, 0)$, $\mathbf{H}=(1/\sqrt{3}, 1/3, a/2c)$. To reach a numerical accuracy exceeding 0.1 for λ requires careful sampling *throughout* the Brillouin-zone for electrons as well as for phonons due to the small size of the cylindrical σ -hole sheets². We therefore used Savrasov's¹⁸ linear-responce full-potential LMTO density-functional method, proven to describe the superconducting and transport properties of *e.g.* Al and Pb with high accuracy. The Brillouin-zone integrations were performed with the full-cell tetrahedron method²² with the \mathbf{k} -points placed on the $(\mathbf{A}, \mathbf{B}, \mathbf{C})/24$ sublattice. For the valence bands, a triple-kappa *spd* LMTO basis set was employed and the Mg $2p$ -semicore states were treated as valence states in a separate energy window. The charge densities and potentials were represented by spherical harmonics with $l \leq 8$ inside the non-overlapping MT spheres, and by plane waves with energies ≤ 201 Ry in the interstitial region.

The resulting electronic structure is practically identical with that of previous calculations^{2–5}. Near and below the Fermi level there are two B p_z π -bands and three quasi-2D B-B bonding σ -bands. The σ and π bands do not hybridize when $k_z=0$ and π/c . The π -bands lie lower with respect to the σ -bands than in graphite and have more k_z -dispersion due to the influence of Mg, the

on-top stacking, and the smaller c/a -ratio. This causes the presence of $p_{\sigma l}=0.056$ light and $p_{\sigma h}=0.117$ heavy holes near the doubly-degenerate top along ΓA of the σ -bands. For the density of states at $\varepsilon_F \equiv 0$, we find: $N(0) = N_{\sigma l}(0) + N_{\sigma h}(0) + N_{\pi}(0) = 0.048 + 0.102 + 0.205 = 0.355$ states/(MgB₂-eV·spin).

The σ and π -bands may be understood and described with reasonable accuracy near ε_F using the orthogonal tight-binding approximation with respectively the B p_z orbitals and the B-B two-center bond-orbitals formed from the B sp^2 hybrids: With two p_z orbitals per cell and hopping between nearest neighbors only ($\varepsilon_z=0.04$ eV, $t_z^\perp=0.92$ eV, and $t_z=1.60$ eV), the π -bands are²: $\varepsilon_\pi(\mathbf{k}) = \varepsilon_z + 2t_z^\perp \cos ck_z \pm t_z \sqrt{1 + 4 \cos(ak_y/2) [\cos(ak_y/2) + \cos(ak_x\sqrt{3}/2)]}$. The bonding σ -band Hamiltonian is:

$$H_\sigma(\mathbf{k}) = t_{sp^2} - 2t_b^\perp \cos ck_z - 2t_b \begin{pmatrix} 0 & \cos \gamma + r \cos(\alpha + \beta) & \cos \alpha + r \cos(\beta + \gamma) \\ c.c. & 0 & \cos \beta + r \cos(\alpha - \gamma) \\ c.c. & c.c. & 0 \end{pmatrix},$$

in the representation of the three bond-orbitals per cell, with t_{sp^2} being the energy of the two-center bond, and the integrals for hopping between nearest and 2nd-nearest bond orbitals in the same layer being respectively $t_b=5.69$ eV and $t_b' \equiv rt_b=0.91$ eV, and with $t_b^\perp=0.094$ eV being an order of magnitude smaller than t_b^\perp . Moreover, $\alpha \equiv \frac{1}{2}\mathbf{k} \cdot \mathbf{a}$, $\beta \equiv \frac{1}{2}\mathbf{k} \cdot \mathbf{b}$, and $\gamma \equiv \frac{1}{2}\mathbf{k} \cdot (\mathbf{b} - \mathbf{a})$. Along ΓA , $\alpha=\beta=\gamma=0$ so that there is a singly-degenerate band of symmetry A with dispersion $t_{sp^2} - 2t_b^\perp \cos ck_z - 4(t_b + t_b')$ and a doubly-degenerate band of symmetry E with dispersion $t_{sp^2} - 2t_b^\perp \cos ck_z + 2(t_b + t_b')$. The E-band is slightly above the Fermi level and its eigenvectors are given in the two inserts at the bottom of Fig. 1. The Fermi-surface sheets are warped cylinders² which may be described by expanding the two upper bands of $H_\sigma(\mathbf{k})$ to lowest order in $k_x^2 + k_y^2 \equiv k_\perp^2$. This yields:

$$\varepsilon_{\sigma n}(\mathbf{k}) = \varepsilon_0 - 2t_b^\perp \cos ck_z - k_\parallel^2/m_{\sigma n}, \quad (2)$$

where $\varepsilon_0 \equiv t_{sp^2} + 2(t_b + t_b') = 0.58$ eV is the average energy along ΓA and the units of $k_\parallel^2/m_{\sigma n}$ and k_\parallel are respectively Ry and a_0^{-1} . The light and heavy-hole masses are respectively $m_{\sigma l} = 4/(t_b a^2) = 0.28$ and $m_{\sigma h} = 4/(3t_b' a^2) = 0.59$ relatively to that of a free electron. For energies so closely below $\varepsilon(\Gamma)$ that Eq. (2) holds, the number-of-states function is $\int k_\parallel^2 n(\varepsilon, k_z) dk_z/k_{BZ}^2 = k_\parallel^2 n(\varepsilon, \pi/2c)/k_{BZ}^2 = (\varepsilon_0 - \varepsilon) m_{\sigma n}/k_{BZ}^2$, and its energy derivative is therefore constant: $N_{\sigma n}(\varepsilon) = m_{\sigma n}/k_{BZ}^2$. Here, $\pi k_{BZ}^2 = (2\pi a_0/a)^2 2/\sqrt{3}$ is the area, and k_{BZ} the average radius of the Brillouin zone. Note that the σ -sheets are quite narrow: $k_{F\parallel l}(\pi/2c)/k_{BZ} = \sqrt{0.056/2} = 0.17$ and $k_{F\parallel h}(\pi/2c)/k_{BZ} = \sqrt{0.117/2} = 0.24$.

The dynamical matrix was calculated for \mathbf{q} -points on the (A, B, C)/6 sublattice using the B-mass 10.811 which corresponds to the natural mix of isotopes. The

phonon dispersions $\omega_m(\mathbf{q})$ and density of states $F(\omega)$ are shown in Fig.1. The agreement between our $F(\omega)$ and those obtained from inelastic neutron scattering^{16,17} is excellent; our peaks at 260 and 730 cm⁻¹ (32 and 90 meV) are seen in the experiments at 32 and 88 meV. For the frequencies of the optical Γ -modes we get: 335 cm⁻¹ (E_{1u}), 401 cm⁻¹ (A_{2u}), 585 cm⁻¹ (E_{2g}), and 692 cm⁻¹ (B_{1g}). These values are in good agreement with those of previous calculations, except for the all-important E_{2g} modes where the LAPW² and pseudo-potential⁴ calculations give values which are respectively ~ 100 cm⁻¹ smaller and larger than ours. These doubly degenerate modes are the optical B-B bond-stretching modes (obs). Close to ΓA , they have exactly the same symmetry and similar dispersions as the light and heavy σ -holes, although with the opposite signs. The E eigenfunctions shown at the bottom of Fig.1 now refer to displacement patterns, e.g., $\{-1, 0, 1\}$ has one bond shortened, another bond stretched by the same amount, and the third bond unchanged. These E displacement patterns will obviously modulate the electronic bond energy, t_{sp^2} , in such a way that the light holes couple to one, and the heavy holes to the other mode, with the same diagonal ($g_{\sigma,obs}$) and no off-diagonal matrix element. An and Pickett⁵ judged that this electron-phonon (e-ph) matrix element will be the dominating one. This, we shall confirm, although we dispute their estimate of λ .

We now turn to the superconducting properties. Since the Fermi surface has two σ and two π -sheets, one might expect anisotropic pairing with different gaps on different sheets. The experimental data^{11,12}, however, demonstrate that a change of residual resistivity corresponding to a change of impurity scattering by two orders of magnitude hardly affects T_c , although T_c for anisotropic pairing is very sensitive to impurity scattering. The relative linewidth of the $m\mathbf{q}$ -phonon due to e-ph coupling is²³:

$$\frac{\gamma_m(\mathbf{q})}{\omega_m(\mathbf{q})} = 2\pi \sum_{nn'\mathbf{k}} \delta[\varepsilon_n(\mathbf{k})] \delta[\varepsilon_{n'}(\mathbf{k} + \mathbf{q})] |g_{n\mathbf{k},n'\mathbf{k}+\mathbf{q},m}|^2 \equiv \pi N(0) \omega_m(\mathbf{q}) \lambda_m(\mathbf{q}),$$

where the factor 2 is from spin degeneracy and $\sum_{\mathbf{k}}$ is the average over the Brillouin zone, so that $N(0) = \sum_{n\mathbf{k}} \delta[\varepsilon_n(\mathbf{k})]$. We have (safely) assumed that $\omega_m(\mathbf{q}) \ll \mathbf{q} \cdot \mathbf{v}_n(\mathbf{k})$, where $\mathbf{v}_n(\mathbf{k}) \equiv \nabla_{\mathbf{k}} \varepsilon_n(\mathbf{k})$ is the electron velocity. The e-ph matrix element is: $g_{n\mathbf{k},n'\mathbf{k}+\mathbf{q},m} = \langle n\mathbf{k} | \delta V | n'\mathbf{k} + \mathbf{q} \rangle / \delta Q_{m\mathbf{q}}$, where the displacement in the i -direction of the j th atom is related to the phonon eigenvector $e_{ij,m\mathbf{q}}$ and displacement $\delta Q_{m\mathbf{q}}$ by: $\delta R_{ij} = e_{ij,m\mathbf{q}} \delta Q_{m\mathbf{q}} / \sqrt{2M_j \omega_{m\mathbf{q}}}$. The Eliashberg spectral function is:

$$\alpha^2(\omega) F(\omega) \equiv \frac{1}{2\pi N(0)} \sum_{m\mathbf{q}} \frac{\gamma_m(\mathbf{q})}{\omega_m(\mathbf{q})} \delta[\omega - \omega_m(\mathbf{q})],$$

and the strength of the e-ph interaction is finally: $\lambda \equiv 2 \int_0^\infty \omega^{-1} \alpha^2(\omega) F(\omega) d\omega = \sum_{m\mathbf{q}} \lambda_m(\mathbf{q})$.

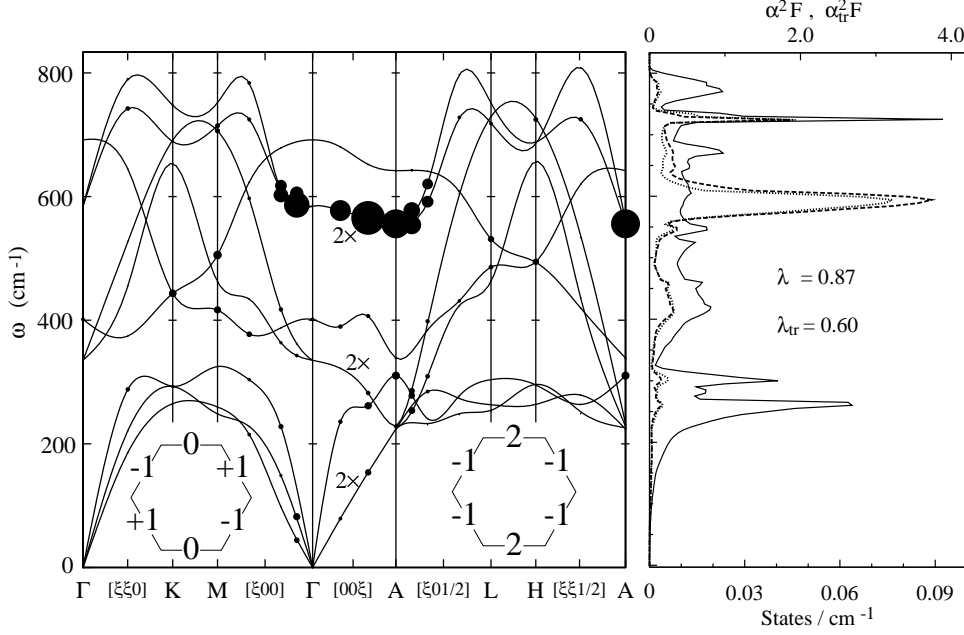


FIG. 1. *Left:* Calculated phonon dispersion curves in MgB₂. The area of a circle is proportional to the mode- λ . The insets at the bottom show the two ΓA E eigenvectors (un-normalized), which apply to the holes at the top of the σ -bands (bond-orbital coefficients) as well as to the optical bond-stretching phonons (relative change of bond lengths). *Right:* $F(\omega)$ (full curve and bottom scale), $\alpha^2(\omega)F(\omega)$ (broken) and $\alpha_{tr}^2(\omega)F(\omega)$ (dotted). See text.

The dominance of the σ - σ coupling via the optical bond-stretching mode is clearly seen in Fig. 1, where the area of a black circle is proportional to $\lambda_m(\mathbf{q})$. Along ΓA , except when $\mathbf{q} \cdot \mathbf{v} < \omega$, only the small k_z -dispersion (t_b^\perp) makes $\lambda_m(\mathbf{q})$ not diverge so that the numerical values are inaccurate due to the relative coarseness our \mathbf{k} -mesh. The nearly cylindrical σ -sheets, whose diameters are of about the same size as the smallest, non-zero q_{\parallel} on the affordable ($\mathbf{A}, \mathbf{B}, \mathbf{C}$)/6-mesh, require even more care in the numerical \mathbf{q} -integration: In case of a single cylindrical sheet with p holes, $\lambda(q_{\parallel})$ has the well-known $\text{Im} \chi(q_{\parallel}, \omega \rightarrow 0)$ -form: $\lambda(q_{\parallel})/\lambda = (2\pi p x \sqrt{1-x^2})^{-1} \theta(1-x)$ with $x=q_{\parallel}/2k_{F\parallel}$. This function vanishes when $q_{\parallel} > 2k_{F\parallel}$, has a flat minimum of value $(\pi p)^{-1}$ near $q_{\parallel} = \sqrt{2}k_{F\parallel}$, and has integrable divergencies at $q_{\parallel} = 2k_{F\parallel}$ and 0. The proper average of $\lambda(q_{\parallel})$ is λ . This means, that $\lambda(\mathbf{q})$ calculated on a coarse mesh scatter violently for small $|\mathbf{q}|$, but that weighting with $\lambda/\lambda(q_{\parallel})$ gives the same, correct result for all these points, provided that warping, as well as \mathbf{k}, \mathbf{k}' -dependence of g and ω , are neglected. In case of two cylindrical sheets, and no coupling between them, $\lambda_n(q_{\parallel})/\lambda_n$ should be weighted by $m_n^2/(m_l^2 + m_h^2)$. In our numerical evaluation of the e-ph interaction with the linear-response code¹⁸ we discarded the values of $\lambda_m(\mathbf{q})$ with \mathbf{q} along ΓA , and added those on the ($\mathbf{A}/12, \mathbf{B}/12, \mathbf{C}/6$)-mesh for which $\sqrt{2}k_{F\parallel l} \lesssim q_{\parallel} \lesssim \sqrt{2}k_{F\parallel h}$. The result was: $\lambda = 0.62 + 0.25$, where 0.62 was the contribution from \mathbf{q} 's so small that σ - σ coupling occurs, and 0.25 was the contribution from

the remaining part of \mathbf{q} -space, which must involve a π -sheet. Had we included the inaccurate $\lambda_m(\mathbf{q})$ -values along the ΓA -line, the σ - σ result would have been 0.72 instead of 0.62. The result was finally checked by using the approximate $\lambda(q_{\parallel})/\lambda$ correction for the point $\mathbf{q} = \mathbf{A}/12$. This yielded 0.58 instead of 0.62. In conclusion: $\lambda = 0.87 \pm 0.05 = (0.62 \pm 0.05) + 0.25 \equiv \lambda_{\sigma} + \lambda_{\pi}$.

The Eliashberg function shown on the right-hand side of Fig. 1 is dominated by the large σ - σ peak around $\omega_{obs} = 590 \text{ cm}^{-1} = 73 \text{ meV}$. The facts that the σ -sheets are narrow, warped cylinders whose coupling is dominated by intra-sheet coupling via the optical bond-stretching mode, and that the coupling between σ - and π -sheets is negligible, lead to the following approximation:

$$\alpha^2(\omega)F(\omega) \approx \alpha_{\pi}^2(\omega)F(\omega) [N_{\pi}(0)/N(0)] + |g_{\sigma,obs}|^2 \delta(\omega - \omega_{obs}) [N_{\sigma l}^2(0) + N_{\sigma h}^2(0)]/N(0),$$

where $\alpha_{\pi}^2(\omega)F(\omega)$ is the usual expression, but with π -electrons only. In An's and Picket's estimate⁵, $\lambda_{\sigma} = 0.95$, a factor $[N_{\sigma l}^2(0) + N_{\sigma h}^2(0)]/N_{\sigma}(0)N(0) = 0.24$ appears to be missing. The rigid-atomic-sphere estimate $\lambda = 0.7$ by Kortus *et al.* is closer to our value 0.87.

Knowing $\alpha^2(\omega)F(\omega)$ and a value of the Coulomb pseudopotential $\mu^*(\omega_c)$, we solve the Eliashberg equation on the real frequency axis²⁵, and obtain $T_c = 40 \text{ K}$ if $\mu^*(\omega_c) = 0.14$. Taking retardation effects into account, we find $\mu^* \equiv \mu^*(\omega_c) / [1 + \mu^*(\omega_c) \ln(\omega_c/\omega_{ln})] = 0.10$, where $\omega_{ln} = 504 \text{ cm}^{-1} = 62 \text{ meV}$ is obtained from: $0 = \int_0^{\infty} \ln(\omega/\omega_{ln}) \omega^{-1} \alpha^2(\omega)F(\omega) d\omega$, and the cut-off frequency is taken as $\omega_c = 10 \max \omega = 8000 \text{ cm}^{-1}$. This value

of μ^* is at the lower end of what is found for simple *sp*-metals¹⁸. The relation back to a screened Coulomb interaction U is: $\mu^* = \mu/[1 + \mu \ln(\omega_p/\omega_{In})]$, where $\mu=UN(0)$ and $\omega_p \sim 7$ eV is the plasma frequency given below. We thus find: $\mu=0.19$ and $U=1.1$ eV, which are normal values. Had we used the approximate McMillan expression (1), the slightly higher value $\mu^*=0.14$ would be needed to reproduce the experimental T_c .

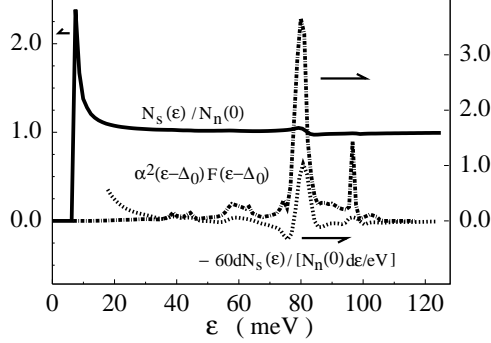


FIG. 2. Normalized density of states (full) and the negative of its energy-derivative (dotted) as obtained from the Eliashberg equation with $\mu^*=0.10$ and $T=3$ K.

In Fig.2 we show our Eliashberg calculation with $\mu^*=0.10$ of the density of states, $N_s(\epsilon)/N(0) = \text{Re} \left[\epsilon / \sqrt{\epsilon^2 - \Delta_{3K}^2(\epsilon)} \right]$, in the superconductor. The BCS singularity is at $\epsilon=\Delta_{3K}(0)=6.8$ meV, which is in accord with the 4.9-6.9 meV found in tunneling experiments⁹. This yields: $2\Delta_0/k_B T_c=3.9$ which is slightly higher than the BCS value of 3.52. The distinct feature near 80 meV corresponds to the peak in $\alpha^2(\omega)F(\omega)$ at 73 meV, shifted by the 6.8 meV gap. The latter function is also shown in the figure together with the measurable quantity $-d^2I/dV^2 \sim -dN_s(\epsilon)/d\epsilon$.

We have calculated the change in T_c upon isotope substitution of ^{11}B for ^{10}B and get: $\delta T_c=-1.7$ K, which corresponds to the exponent $-\delta \ln T_c/\delta \ln M_B=0.46$. This agrees well with the measured⁸ value: $\delta T_c=-1$ K. For the change of the gap, which may be measured in tunnelling and optical experiments, we calculate: $\delta \Delta_0=-1.9$ cm⁻¹, which corresponds to the exponent $-\delta \ln \Delta_0/\delta \ln M_B=0.38$.

Finally, we have considered transport properties in the normal state. Here, solution of the kinetic equation leads to the transport e-ph spectral function $\alpha_{tr,x}^2(\omega)F(\omega)$, and similarly for y and z . These components are given by the previous expressions, but with the additional factor $[v_{nx}^2(\mathbf{k}) - v_{nx}(\mathbf{k})v_{nx}(\mathbf{k}+\mathbf{q})]/\langle v_x^2 \rangle$ inserted. $\langle v_x^2 \rangle \equiv N(0)^{-1} \sum_{n\mathbf{k}} v_{nx}^2(\mathbf{k}) \delta[(\epsilon_n(\mathbf{k}))]$. In Fig. 1 the directional average, $\alpha_{tr}^2(\omega)F(\omega)$, is seen to have the same shape as $\alpha^2(\omega)F(\omega)$, except for the σ - σ interaction via the optical bond-stretching modes, whose $\alpha_{tr}^2(\omega)F(\omega)$ is smaller, presumably due to the near two-dimensionality of the σ -bands. As a re-

sult, $\lambda_{tr} = 0.60$. For the plasma frequencies, $\omega_{p,x}^2 = 4\pi e^2 N(0) \langle v_x^2 \rangle / [\mathbf{abc}]$, we find: $\omega_{p,x}=\omega_{p,y}=7.02$ eV and $\omega_{p,z}=6.68$ eV. Also the temperature dependence of the specific dc-resistivity calculated with the standard Bloch-Grüneisen expression, $\rho_{dc,x}(T) = (\pi/\omega_{p,x}^2 T) \int_0^\infty \omega \sinh^{-2}(\omega/2T) \alpha_{tr,x}^2(\omega)F(\omega)d\omega$, is nearly isotropic and, as shown in Fig.3, is in accord with recent measurements on dense wires¹² over the entire temperature range. The crossover from power-law to linear temperature dependence is seen to occur near $\max \omega/5=160$ cm⁻¹=230 K, as expected²⁴.

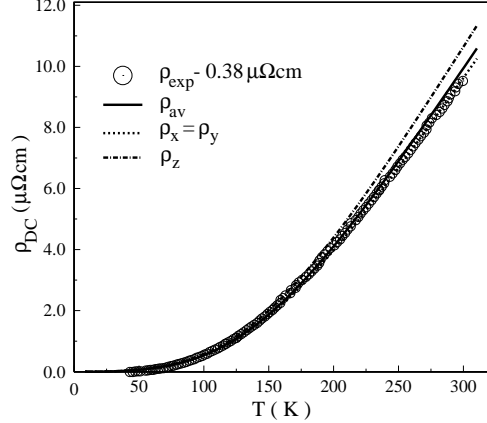


FIG. 3. Calculated dc-resistivities in different directions compared with the experiment in Ref. 12.

In conclusion, we have presented an accurate *ab initio* calculation of the e-ph interaction in MgB₂ and find $\lambda = 0.87 \pm 0.05$. Eliashberg theory with $\mu^*=0.10$ gives good agreement with available experiments and several predictions. The unexpected high T_c is due to the large λ -value caused by the presence of holes in the B-B bonding σ -band and the relative softness of the optical bond-stretching modes. MgB₂ thus seems to be a simple and clear case of an intermediate-coupling e-ph pairing *s*-wave superconductor.

Useful discussions with R. K. Kremer, I. I. Mazin, S. Savrasov, D. Savrasov, and S. V. Shulga are acknowledged.

-
- ¹ J. Nagamatsu, N. Nakagawa, T. Muranaka, Y. Zenitani, and J. Akimitsu, *Nature* **410**, 63 (2001).
 - ² J. Kortus, I.I. Mazin, K.D. Belashchenko, V.P. Antropov, and L.L. Boyer, *cond-mat/0101446*.
 - ³ K.D. Belashchenko, M. van Schilfhaarde, and V.P. Antropov, *cond-mat/0102290*.
 - ⁴ G. Satta, G. Profeta, F. Bernardini, A. Continenza, and S. Massidda, *cond-mat/0102358*.
 - ⁵ J.M. An and W.E. Pickett, *cond-mat/0102391*.

- ⁶ C.T. Chan, K.M. Ho, and W.A. Kamitakahara, Phys. Rev. B **36**, 3499 (1987).
- ⁷ O. Gunnarsson, Rev. Mod. Phys. **69**, 575 (1997).
- ⁸ S.L. Bud'ko, G. Lapertot, C. Petrovic, C.E. Cunningham, N. Anderson, and P.C. Canfield, Phys. Rev. Lett. **86**, 1877 (2001).
- ⁹ A. Sharoni, I. Felner, and O. Millo, cond-mat/0102325.
- ¹⁰ D.K. Finnemore, J.E. Ostenson, S.L. Bud'ko, G. Lapertot, and P.C. Canfield, Phys. Rev. Lett. **86**, 2420 (2001).
- ¹¹ C.U. Jung, M.-S. Park, W.N. Kang, M.-S. Kim, S.Y. Lee, and S.-I. Lee, cond-mat/0102215.
- ¹² P.C. Canfield, D.K. Finnemore, S.L. Bud'ko, J.E. Ostenson, G. Lapertot, C.E. Cunningham, and C. Petrovic, Phys. Rev. Lett. **86**, 2423 (2001).
- ¹³ S.L. Bud'ko, C. Petrovic, G. Lapertot, C.E. Cunningham, and P.C. Canfield, cond-mat/0102413.
- ¹⁴ R.K. Kremer, B.J. Gibson, and K. Ahn, cond-mat/0102432.
- ¹⁵ Ch. Wälti, E. Felder, C. Degen, G. Wigger, R. Monnier, B. Delly, and H.R. Ott, cond-mat/0102522.
- ¹⁶ T.J. Sato, K. Shibata, and Y. Takano, cond-mat/0102468.
- ¹⁷ R. Osborn, E.A. Goremychkin, A.I. Kolesnikov, and D.G. Hinks, cond-mat/0103064.
- ¹⁸ S.Y. Savrasov, Phys. Rev. B **54**, 16470 (1996); S.Y. Savrasov and D.Y. Savrasov, *ibid*, 16487.
- ¹⁹ S.H. Vosko, L. Wilk and M. Nusair, Can. J. Phys. **58**, 1200 (1980).
- ²⁰ J.P. Perdew, K. Burke and M. Ernzerhof, Phys. Rev. Lett. **77**, 3865 (1996).
- ²¹ A. Lipp and M. Roder, Z. Anorg. Chem. **334**, 225 (1966).
- ²² P.E. Blöchl, O. Jepsen, and O.K. Andersen, Phys. Rev. B **49**, 16223 (1994)
- ²³ P.B. Allen and B. Mitrović, *Solid State Physics*, **37**, 1 (1982).
- ²⁴ P.B. Allen, T.P. Beaulac, F.S. Khan, W.H. Butler, F.J. Pinski, and J.C. Swihart, Phys. Rev. B **34**, 4331 (1986).
- ²⁵ S.V. Shulga (unpublished).